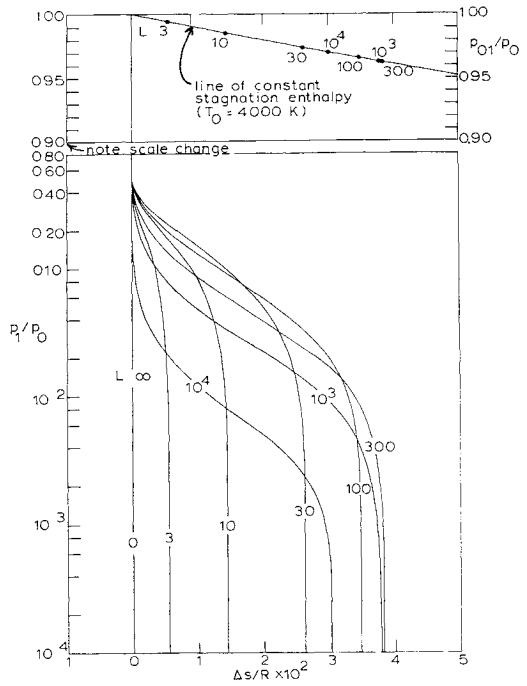

Fig 1 Entropy production as a function of freestream pressure for various values of the parameter L

ation as a function of pressure ratio during the expansion process for various values of L

The limiting cases of equilibrium ($L = \infty$) and frozen flow ($L = 0$) appear as vertical lines on Fig 1, since such expansions are isentropic In each case involving nonequilibrium, the expansion proceeds initially in equilibrium up through the throat with no entropy change, then goes through a region of nonequilibrium during which entropy is produced, and finally freezes with no further entropy increase It should be noted that, for small values of L, the entire flow is nearly frozen, and the total entropy increase is small As L is increased to intermediate values, the portion of the flow in which nonequilibrium exists increases, and thus the entropy produced is greater For large values of L, the flow is closer to equilibrium, and the total entropy produced is less (For the lowest values of L, the possibility exists of the flow freezing upstream of the throat and altering the results somewhat However, the trend indicated by the present analysis should still apply)

An appreciation of the consequences of entropy production in the nozzle can be gained by considering its effect on freestream total pressure $p_{0\,1}$ The freestream total pressure is defined as the pressure that would exist if the flow at freestream conditions could be compressed isentropically to an equilibrium state with a zero velocity (i e , to the total enthalpy based on equilibrium) This imaginary compression could be thought of as taking place by the following two-step process Starting from a nonequilibrium state in the freestream, the gas first undergoes a frozen isentropic compression ($d\sigma = 0$) to the point at which $T = T$ The remainder of the compression is carried out isentropically in equilibrium ($T = T$)

The freestream total pressure $p_{0\,1}$ can be determined from Fig 1 for any freestream condition by following a constant-entropy path up to the line of constant stagnation enthalpy The points indicated on the line of constant stagnation enthalpy show the maximum reduction in $p_{0\,1}$ for the various values of L For the conditions investigated, the loss in freestream total pressure due to nonequilibrium can be as great as 4%, as shown for the case $L = 300$

Additional calculations were made to compare the pitot pressure p_0' of a nonequilibrium nozzle flow to that of an equilibrium nozzle flow with identical stagnation conditions and area ratios In these calculations, equilibrium flow was assumed to exist behind the shock It was found that a lower pitot pressure p_0' is always observed for the nonequilibrium case This drop in p_0' is of somewhat smaller proportions than the drop in $p_{0\,1}$, but no explicit relationship between the two is available

However, the freestream conditions at any point along the nozzle axis can be calculated as was done in Ref 1, and all entropy production, or nonequilibrium effects, in the nozzle will be reflected in these freestream quantities Using these freestream values and applying the conservation equations across the shock, the properties behind the shock can be calculated using a simple iterative procedure In addition, if the flow behind the shock is assumed to be in equilibrium, the pitot pressure can easily be calculated

References

[1] Erickson, W D , "Vibrational-nonequilibrium flow of nitrogen in hypersonic nozzles," NASA TN D 1810 (1963)

[2] Treanor, C E and Marrone, P V , "The effect of dissociation on the rate of vibrational relaxation," Cornell Aeronaut Lab Inc Rept QM 1626-A-4 (February 1962)

[3] Presley, L L , private communication, Ames Research Center (January 1963 and June 1963)

[4] Vincenti W G , lectures on physical gas dynamics, Stanford Univ (1961)

Sandwich Cylinder Instability under Nonuniform Axial Stress

R A Gellatly* and R H Gallagher†
Textron's Bell Aerosystems Company, Buffalo, N Y

THIS note is concerned with the prediction of the elastic instability of an axially loaded sandwich cylinder of mean radius r and core thickness h, with isotropic faces of equal thickness t (Fig 1) The faces possess only in-plane stiffness and have a modulus of elasticity E, whereas the core possesses only a transverse shear stiffness with a modulus of rigidity G The axial load per unit circumferential length, N_x, varies in the circumferential (y) direction, and at any point the stress in each of the two faces is assumed equal at a value $\sigma_x = N_x/2t$ Conditions of circumferentially varying stress as shown here may result from the combination of an applied axial load and bending moment, or as a result of temperatures that vary around the circumference of the cylinder

The problem of the elastic instability of an isotropic thin-walled cylinder under circumferentially varying axial stress was solved in Refs 1 and 2 on the basis of small-deflection theory Both references concluded that instability is reached when the maximum axial stress has the value

$$\sigma \approx 0\,6Et/r \qquad (1)$$

regardless of the nature of the circumferential variation of σ_x (The compression zone within which the maximum value σ_{cr} occurs must at least extend over the wavelength of a circumferential buckle, however) The wall thickness of the isotropic shell is t Equation (1) is, of course, the small-deflection theory solution for uniform compression In view of these results it would appear reasonable to expect that for the

Received December 10, 1963 Work described in this note was performed as part of an FAA sponsored, ASD-administered study, Contract AF33(657) 8936

* Structures Research Engineer, Aerospace Engineering Department

† Chief, Advanced Airframe Analysis Associate Fellow Member AIAA

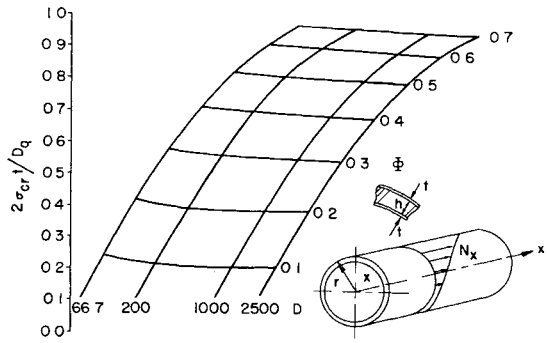

Fig 1 Critical reference stress as a function of stiffness

case of a sandwich cylinder the same conclusions would prevail, i e , the instability stress is given by the solution for uniform axial compression, regardless of how nonuniformly the stress might vary

To develop solutions for the present case, the finite-difference technique used in Ref 1 was applied to Donnell's equation as modified to provide applicability to sandwich cylinders (see Ref 3) A computer program for the subject problem was coded, and on the basis of 20 intervals on the circumference, parametric results were developed Details of this work are given in Ref 4

For sandwich cylinders, two stiffness parameters (D and Φ) are required for a nondimensionalized representation of results These parameters are defined as

$$D = D_q r^2/D \tag{2}$$

and

$$\Phi = Et/G\,r \tag{3}$$

where D is the sandwich flexural stiffness and D_q is the shear stiffness

The specific load conditions studied were those of a linear variation described by the ratio (S) of the crown stress (σ_x) to the stress at the bottom of the cylinder (σ_{xb}) Results were obtained for S = 1 0, 0 5, 0, −0 5, and −1 0 for various combinations of D and Φ

Selected results are tabulated below As anticipated, the critical stresses for nonuniform stress states are effectively equal to the critical stress for uniform axial compression (S = 1 0) The negligible differences between the results for a given stiffness condition may be the result of the differences in stress distribution, but it is also possible that the discrepancies are due entirely to numerical error This question cannot be resolved by use of the present method of solution

Results are plotted in Figs 1 and 2 Figure 1 is a carpet plot wherein both stiffness parameters play a role in the definition of the critical stress If a conventional plotting procedure and slightly altered scales are adopted, as in Fig 2, the parameter D loses its significance, and all results can be approximated by a single line This manner of representation

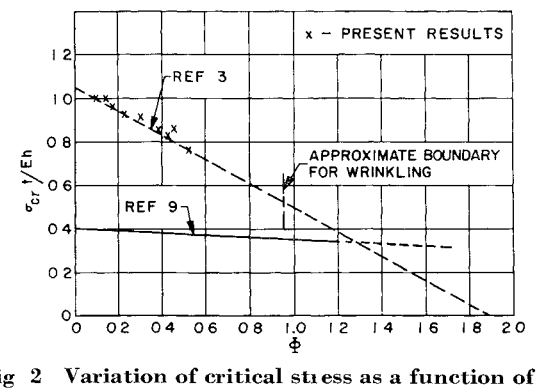

Fig 2 Variation of critical stress as a function of Φ

Table 1 Sandwich cylinder instability stresses

Stiffness parameters		$2\sigma\ t/D_q$ (computed)				
D	Φ	S = −1 0	S = −0 5	S = 0	S = 0 5	S = 1 0[a]
1000	13 49	0 2672	0 2669	0 2665	0 2660	0 2630
200	30 17	0 5536	0 5511	0 5476	0 5433	0 5345
66 7	45 24	0 7699	0 7630	0 7555	0 7450	0 7243

[a] Uniform compression

was also adopted in Refs 3, 5, and 6 The curve presented in Fig 2, based on an equation from Ref 5, is given by

$$\sigma = Eh/r\ [1\ 05 - (Et/1\ 8rG)] \tag{4}$$

The present results, as shown by individual points, are in very good agreement with the foregoing curve

Cylinder elastic instability of the type examined here is limited, in the case of sandwich cylinders, by a wrinkling failure characterized by shear instability of the core This instability is governed by the condition $2\sigma_c\ t/D_q = 1$, and is represented in Fig 2 by a value of $\Phi \approx 0\ 95$

For isotropic cylinders, results obtained from small-deflection theory analyses are in extreme disagreement with test data except when a sufficiently high internal pressurization is applied, the attainable critical stress being extremely sensitive to initial imperfections (e g , out of roundness, etc) It appears reasonable to expect that sandwich cylinder critical stresses will be in closer agreement with small-deflection theory predictions since the initial imperfection effects, which are a function of the radial imperfection magnitude-to-total wall thickness ratio, will be very small in carefully fabricated sandwich cylinder

Experimental results presented by Cunningham and Jacobson[7] lend credence to the foregoing hypothesis On the other hand, the test data of Norris and Kuenzi[8] support the view that large-deflection formulations must be used for the development of design data A design curve from Ref 9, based on large-deflection theory, is reproduced in Fig 2 Note the large differences between the predictions based on large- and small-deflection theory Unquestionably, a rational basis for the design of sandwich cylinders for conditions treated here requires a correlation and critical evaluation of existing test data with the performance of additional tests in regions of the governing parameter Φ which have not yet been examined, and implementation by a theoretical study based on large-deflection theory

It is of interest to note that computed axial wavelengths were found to be essentially independent of the shape of the stress distribution and in agreement with data presented in Ref 5 The wavelength-to-radius ratios were relatively small Thus, the present results should apply to short as well as to long cylinders

References

[1] Bijlaard, P P and Gallagher, R H , "Elastic instability of a cylindrical shell under arbitrary circumferential variation of axial stress," J Aerospace Sci **27,** 854–859 (1960)

[2] Abir, D and Nardo, S V , "Thermal buckling of circular cylindrical shells under circumferential temperature gradients," J Aerospace Sci **26,** 803–808 (1959)

[3] Stein, M and Mayers, J , 'Compressive buckling of simply supported curved plates and cylinders of sandwich construction,' NACA TN 2601 (1952)

[4] Gellatly, R A and Gallagher, R H , "Thermal stress determination techniques for supersonic transport aircraft structures Part II Design data for sandwich plates and cylinders under applied loads and thermal gradients," Aeronaut Systems Div ASD-TDR63-783 (in press)

[5] Teichmann, F K , Wang, C-T, and Gerard, G , "Buckling of sandwich cylinders under axial compression," J Aeronaut Sci **18,** 398–406 (1951)

[6] Leggatt, D M A and Hopkins, H G, "Sandwich panels and cylinders under compressive end loads," Aeronaut Res Council, R and M 2282 (1942)

[7] Cunningham, J H and Jacobson, M J, "Design and testing of honeycomb sandwich cylinders under axial compression," NASA TN D-1510 (1962)

[8] Norris, C B and Kuenzi, E W, "Buckling of long thin plywood cylinders in axial compression, experimental treatment ' U S Forest Products Lab Rept 1322-B (1943)

[9] March, H W and Kuenzi, E W, "Buckling of cylinders of sandwich construction in axial compression," U S Forest Products Lab Rept 1830 (1957)

Sputtering in the Upper Atmosphere

D McKeown* and M G Fox†
General Dynamics/Astronautics, San Diego, Calif

J J Schmidt‡
Air Force Cambridge Research Laboratories, Sunnyvale, Calif

and

D Hopper§
Lockheed Missiles and Space Company, Sunnyvale, Calif

MEASUREMENTS have been made on the sputtering rates of surfaces in the upper atmosphere The measurements were carried out on two Air Force satellites that orbited at about 200 km above the earth At this altitude a satellite sweeps out an intense beam of molecules from the upper atmosphere which impact with energies ranging up to about 10 ev We are studying these impacts to determine the sputtering effects they will have on surfaces

On these two flights, sputtering measurements were made on Au and Ag surfaces Laboratory studies at 30 ev,[1] the lowest energy at which we have been able to make sputtering measurements, show that these two metals have the highest sputtering yield of any materials investigated Hence, knowing the yields for these two metals in the upper atmosphere would place a limit on the yield for other surfaces

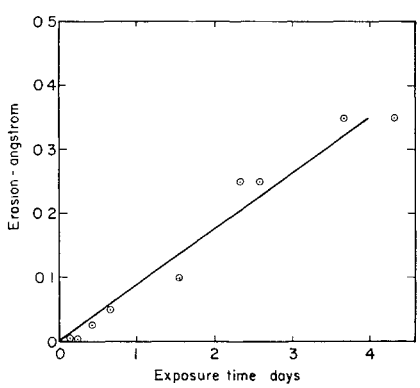

Fig 1 Erosion of Au in the upper atmosphere

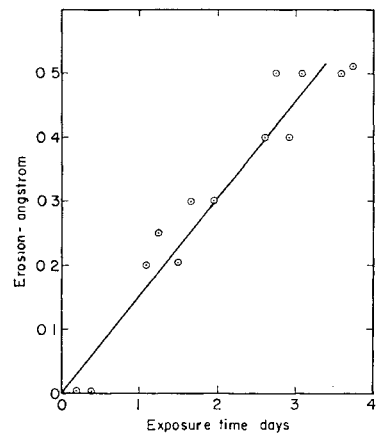

Fig 2 Erosion of Ag in the upper atmosphere

The crystal-oscillator method was used in the measurements The material to be studied is plated on a quartz crystal, and the rate at which it is sputtered off by particle impacts was determined from the change in the oscillator frequency This method for measuring small mass changes has been previously described [2 3] With it, it is possible to measure the average erosion of 0 01Å from a surface

The total thickness of gold eroded from a surface as a function of exposure time in the upper atmosphere is shown in Fig 1 This erosion measurement was made for the air stream impacting a 30° angle relative to the plane of the surface The erosion rate for a gold surface as determined from Fig 1 is 0 1 ± 0 05 Å/day

The total thickness of silver eroded from a surface as a function of exposure time is shown in Fig 2 Here the measurement was made for the air stream impacting at normal incidence to the plane of the surface The erosion rate for a silver surface as determined from Fig 2 is 0 15 ± 0 05 Å/day

From the erosion rate for a surface, one can calculate its sputtering yield in the upper atmosphere [3] The composition of the upper atmosphere is mainly N_2,[4] and one finds the sputtering yield μ in Au atoms ejected per incident N_2 molecule to be

$$\mu \approx 1 \times 10^{-6}\ \mathrm{Au/N_2}$$

This yield occurs at 9 ev, the energy of impact of N_2 on a satellite at 200 km

The sputtering yield for Au as measured here is within a factor of two of that measured on Discoverer 26 [2] The measurement on Discoverer 26 was to determine the sputtering yield of Au for a surface positioned at normal incidence to the air stream As a result of these two measurements, it can be concluded that there is no significant difference in the erosion of a surface as a function of its angle to the air stream

The sputtering yield for Ag as determined from the data given in Fig 2 is

$$\mu \approx 2 \times 10^{-6}\ \mathrm{atoms/N_2}$$

The higher yield for an Ag over that of Au is in agreement with laboratory measurements at higher energies [1] The Ag surface flown on the satellite had been exposed to the atmosphere at the launch site for several days prior to launch, and it most probably had reacted with sulfur compounds in the air to form Ag_2S This layer of Ag_2S would have sputtered at a greater rate than Au because of the more optimum transfer of energy to Ag_2S by N_2

The energy transfer coefficient is $4m_1m_2/(m_1 + m_2)^2$, where m_1 is the molecular weight of the impacting particle, and

Received December 16, 1963 The research reported in this paper was sponsored in part by the Air Force Missile Development Center, Air Force Systems Command, under Contract AF29(601) 5997, and the Office of Naval Research, Contract 3157(00) Satellite flights were carried out under the auspices of the Air Force System Division and the Air Force Cambridge Research Center The authors wish to thank L L Letterman, F W Groesbeck, J H Miller, D Sprague, and J R Talley for their generous help, needed in the making of these measurements

* Head, Satellite Surface Physics Group, Space Science Laboratory Associate Fellow Member AIAA

† Development Engineer, Satellite Surface Physics Group

‡ Staff Scientist, Resident Scientist Office

§ Flight Test Analytical Engineer